HTML ABSTRACT • LINKS

Stress map for ion irradiation: Depth-resolved dynamic competition between radiation-induced viscoelastic phenomena in SiO_2

T. van Dillen, M. Y. S. Siem, and A. Polman[a)]
FOM-Institute for Atomic and Molecular Physics, Kruislaan 407, NL-1098 SJ Amsterdam, The Netherlands

(Received 5 January 2004; accepted 21 May 2004)

The dynamic competition between structural transformation, Newtonian viscous flow, and anisotropic strain generation during ion irradiation of SiO_2, leads to strongly depth-dependent evolution of the mechanical stress, ranging between compressive and tensile. From independent *in situ* stress measurements during irradiation, generic expressions are derived of the nuclear stopping dependence of both the structural transformation rate and the radiation-induced viscosity. Using these data we introduce and demonstrate the concept of a "stress map" that predicts the depth-resolved saturation stress in SiO_2 for any irradiation up to several MeV. © *2004 American Institute of Physics*. [DOI: 10.1063/1.1773927]

Ion irradiation is a widely used technique to modify the structure and composition of thin film materials. It is the key doping technology in integrated circuit manufacturing and is used to locally modify and tailor optical, magnetic, or mechanical properties of a wide range of materials. Over the past years, ion irradiation has enabled a large number of important fundamental and technological innovations.

Ion irradiation can induce large changes in the mechanical stress state of a material. Surprisingly, this effect has only been marginally studied.[1–3] However, mechanical stress is known to affect important parameters such as thin film stability, impurity diffusion, optical birefringence, and many other properties. Ion irradiation of amorphous SiO_2 causes a reduction in the mean Si–O–Si bridging bond angle, leading to a new structural state with a higher equilibrium density.[4] This leads to the buildup of a tensile stress if the irradiated film is constrained on a substrate. Second, stress relaxation by ion irradiation-induced Newtonian viscous flow occurs,[3,5] and third, the relaxation of shear stresses that are brought about by the expansion of the highly anisotropic ion-induced thermal spike, causes anisotropic strain that freezes in as the thermal spike cools down.[6] This results in the buildup of a compressive stress if the film is constrained on a substrate.

In the past we have developed a qualitative model to describe the stress evolution in SiO_2 during ion irradiation, taking into account the interplay between these three ion irradiation-induced processes. Even though this model appears successful,[3] it is only a rough approximation and its applicability is limited, since it does not take into account the depth dependence of each of the radiation-induced effects in the film. However, each of the three effects strongly depends on either the nuclear or electronic energy loss (stopping), which are both highly depth dependent.

In this letter we evaluate the depth dependence of the local stress in SiO_2 due to the depth-dependent stopping. We demonstrate that the local stress shows variations with depth as large as several hundred MPa, even ranging between compressive and tensile. Using this model it now becomes possible to construct a "stress map" that can be used to predict the local saturation stress in SiO_2 for any ion/energy combination. In our analysis we limit ourselves to ion energies up to a few MeV, where electronic stopping effects on densification and flow are negligible.

As a starting point we use the solution of a differential equation that describes the interplay between the three ion irradiation-induced processes[3,7] and gives the stress as a function of ion fluence:

$$\sigma(\phi) = Y_{ox}\left[(-\varepsilon_1+\varepsilon_{\text{sat}}-C)\cdot\exp\left(-\frac{Y_{ox}}{6\eta_{\text{rad}}}\phi\right) + C\exp\left(-\frac{\phi}{\phi_s}\right)-\varepsilon_{\text{sat}}\right], \quad (1)$$

where $C=6\eta_{\text{rad}}(\varepsilon_2-\varepsilon_1)/(6\eta_{\text{rad}}-Y_{ox}\phi_s)$ and $\varepsilon_{\text{sat}}=-6A\eta_{\text{rad}}/Y_{ox}$ with Y_{ox} the biaxial stress state modulus of SiO_2. Here, we have assumed a damage overlap model for structural transformation, where the in-plane strain evolves exponentially from ε_1 to ε_2 with a characteristic fluence ϕ_s, Newtonian viscous flow with a radiation-induced viscosity η_{rad} and anisotropic strain generation at a constant rate A.

Next, we take into account the stopping dependence of the parameters ϕ_s, η_{rad}, and A in SiO_2. Experiments by Devine *et al.* have shown that structural transformations occur at a characteristic fluence: $\phi_s=\kappa F_n^{-\lambda}$, with F_n the nuclear stopping.[4] Our previous measurements have shown that the radiation-induced viscosity decreases with F_n as: $\eta_{\text{rad}}=\alpha F_n^{-\delta}$.[3] Benyagoub and others have shown that the anisotropic strain generation rate A increases linearly with electronic stopping (F_e) above a threshold:[8] $A=c\times(F_e-F_{th})$, with $c=3.38\times10^{-17}$ cm$^2\times$nm/keV. Using these parameters, $F_{th}=0.6$ keV/nm, and Eq. (1) we can now calculate the fluence dependence of the local stress at each depth z, with the depth-dependent stopping $F_e(z)$ and $F_n(z)$ as input.

Figure 1(a) shows $F_e(z)$ and $F_n(z)$ for 2 MeV Ar irradiation of a SiO_2 film on Si calculated using SRIM, a Monte Carlo simulation program. Fig. 2(a) shows the corresponding local stress as a function of Ar ion fluence for three different depths, calculated using Eq. (1) and characteristic parameters as will be discussed later on. The solid line in Fig. 2(a) represents the local stress at the surface of the film ($z=0$). The initial stress, before irradiation, is taken to be compressive at the experimental value of 260 MPa. It is due to the

a)Electronic mail: polman@amolf.nl

 © 2004 American Institute of Physics

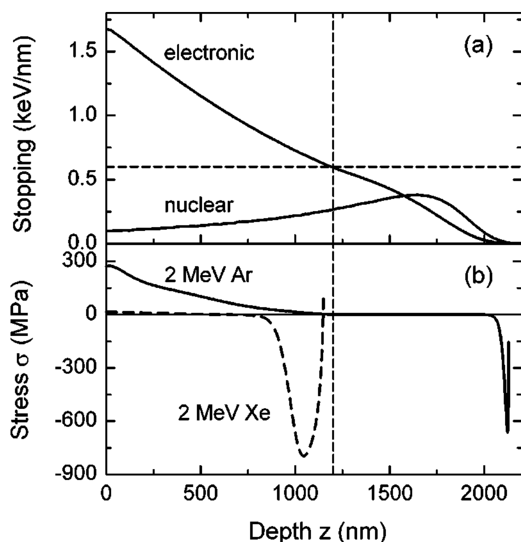

FIG. 1. (a) Electronic and nuclear stopping as a function of the depth for 2 MeV Ar irradiation of SiO_2. The threshold stopping for anisotropic strain generation (F_e=0.6 keV/nm) and the corresponding depth (1200 nm) are indicated by the dashed lines; (b) local stress as a function of depth for 2 MeV Ar (7×10^{14} Ar/cm^2, solid line) and 2 MeV Xe (1×10^{14} Xe/cm^2, dashed line) irradiation of SiO_2.

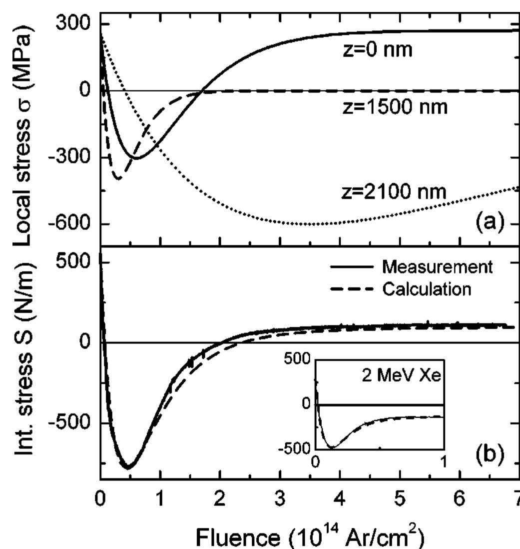

FIG. 2. (a) Local stress as a function of fluence, calculated using Eq. (1), for 2 MeV Ar irradiation of SiO_2 at three different depths indicated in the figure; (b) *in situ* measurement of the integrated stress S as a function of ion fluence during 2 MeV Ar irradiation of SiO_2 at 115 K (solid line). The dashed line represents a calculation of the local stress model by integrating Eq. (1). The inset in (b) shows an *in situ* measurement of the integrated stress (in N/m) in a SiO_2 film as a function of ion fluence during 2 MeV Xe irradiation at 115 K (solid line). The fluence ranges from 0 to 1×10^{14} Xe/cm^2. A calculation by the local stress model using integration of Eq. (1) is also included (dashed line).

difference in thermal contraction between the SiO_2 film and the Si substrate upon cooling down the substrate to room temperature after thermal oxidation at 1050 °C.[3] Upon irradiation the near-surface stress first changes from compressive to tensile. This is due to the structural changes that compact the silica network. After a maximum tensile stress is reached, the stress relaxes due to Newtonian viscous flow. Ultimately, a compressive saturation stress as high as 270 MPa is reached. This saturation stress is a result of a dynamic competition between compressive anisotropic stress generation (with strain rate A) and stress relaxation due to Newtonian viscous flow (with viscosity η_{rad}) and amounts to $6A\eta_{rad}$ [the high-fluence limit of Eq. (1)]. The large saturation stress near the surface results from the high anisotropic strain rate due to the high electronic stopping (high incoming ion energy), and the high viscosity due to the relatively small nuclear stopping [see Fig. 1(a)].

An entirely different behavior is observed deeper in the film, at z=1500 nm [dashed curve in Fig. 2(a)]. At this depth the electronic stopping is below the threshold for anisotropic strain generation and the high-fluence limit of Eq. (1) is zero. Stress relaxation at this depth occurs slightly faster than at the surface due to the higher nuclear stopping. Figure 2(a) also shows the stress evolution at the end-of-range of the ions (z=2100 nm, dotted line) where the nuclear stopping is small and structural changes and radiation-induced flow therefore occur at a slower rate, as is observed in the calculation.

From Fig. 2(a) we can immediately conclude that at a fixed fluence the local stress is strongly dependent on the depth in the irradiated film. For example, at a fluence of 3×10^{14} Ar/cm^2, the surface stress is highly compressive (200 MPa) while at the end-of-range the stress is highly tensile (−600 MPa). Such giant stress inhomogeneities in thin films under ion irradiation have never been considered. To further illustrate the depth dependence of the stress, Fig. 1(b) plots the local stress as a function of depth for 2 MeV Ar irradiation at a fluence of 7×10^{14} ions/cm^2 (solid line). A high compressive stress is seen just below the surface, the stress then decreases with depth and finally vanishes at 1200 nm. The latter is the depth at which the electronic stopping is below the threshold for anisotropic strain generation [see dashed lines in Fig. 1(a)]. At the end-of-range of the ions, around 2100 nm, a narrow tensile stress region is observed, as explained above.

Figure 2(b) shows a measurement (solid line) of the integrated in-plane stress S as a function of the ion fluence during 2 MeV Ar irradiation of a 2.5 μm thick thermally grown SiO_2 film on a 150 μm thick Si(100) substrate at a temperature of 115 K. These data were taken using an *in situ* wafer curvature technique[2] that probes the integrated stress rather than the local stress in the film. Since our model provides the local stress at each depth, we can calculate the depth-integrated stress at any fluence. This calculation is also shown in Fig. 2(b) (dashed line). As can be seen, the calculation corresponds closely with the measurement.

In fitting our model we have optimized the functions $\phi_s=\kappa F_n^{-\lambda}$ and $\eta_{rad}=\alpha F_n^{-\delta}$ to obtain good agreement for three independent measurements of the integrated stress as a function of fluence (1 MeV Ne, 2 MeV Ar, and 2 MeV Xe) using an iteration procedure. Note that the three irradiations, with very different ion masses, lead to entirely different depth profiles of F_e and F_n. These three different measurements were all fitted using the same set of input functions for ϕ_s and η_{rad}: ϕ_s(ions/cm^2)$=1.46\times10^{13}\,F_n^{-0.55}$ and η_{rad}(Pa ion/cm^2)$=1.79\times10^{23}\,F_n^{-0.83}$, with F_n in units of keV/nm. Exponents smaller than unity have been observed by Griscom *et al.*,[9] and may point to defect reactions during ion irradiation.

As an illustration of how these generic expressions consistently describe entirely different experiments, we show in the inset of Fig. 2(b) a measurement of the integrated stress as a function of fluence during 2 MeV Xe irradiation of a

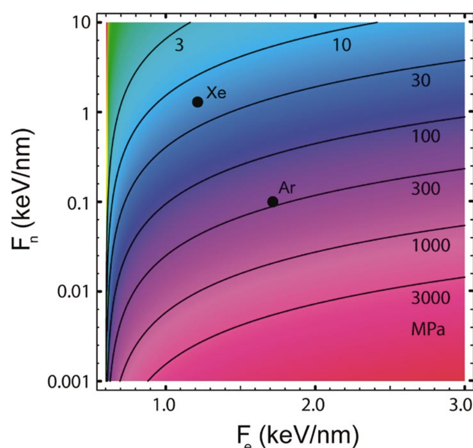

FIG. 3. (Color) Stress map of SiO_2 at 115 K under ion irradiation. Plotted are iso-stress curves of the high-fluence saturation stress $\sigma_{SAT}=6A\,\eta_{rad}$ (values indicated in units of MPa) as a function of the electronic stopping F_e and the nuclear stopping F_n. The near-surface saturation stress ($z=0$ nm) for 2 MeV Ar and 2 MeV Xe irradiation is also shown (closed circles).

SiO_2 film on Si performed at 115 K (solid line). The stress curve exhibits a totally different behavior than for 2 MeV Ar irradiation; the most striking difference is the apparent high-fluence saturation stress that is now tensile. Nevertheless, the calculation [dashed line in the inset of Fig. 2(b)] performed using the same set of input functions as used for the calculation of the 2 MeV Ar irradiation shows very good agreement with the measurement.

This analysis now provides a consistent explanation for the tensile saturation stress that had remained controversial and unexplained to date. This tensile stress now naturally follows from our model as can be seen in Fig. 1(b), which shows the local stress as a function of depth for 2 MeV Xe irradiation at a fluence of 1×10^{14} Xe/cm^2 (dashed line). Clearly, the large ion straggle for Xe leads to a broad tensile contribution at the end-of-range, thus leading to a tensile integrated stress.

Finally, by analogy of the deformation mechanism map that predicts stress–strain-temperature behavior for materials, we introduce the new concept of a "stress map" for ion irradiation. Since the anisotropic strain generation rate A depends on the electronic stopping F_e, and the radiation-induced viscosity η_{rad} on the nuclear stopping F_n, the saturation stress $\sigma_{sat}=6A\,\eta_{rad}$ can be calculated for any irradiation condition. These data can be plotted on a stress map in which iso-saturation stress contours are plotted versus F_e and F_n, as is shown in Fig. 3. For F_e below 0.6 keV/nm the saturation stress vanishes. It can immediately be seen that a high electronic energy loss and a small nuclear energy loss results in a high local saturation stress. In contrast, a small value of the saturation stress occurs in regions where F_n is high and F_e small.

For comparison, the solid dots in Fig. 3 indicate the calculated near-surface saturation stress for 2 MeV Ar and 2 MeV Xe irradiations, taken from Fig. 1(b). The 2 MeV Ar irradiation results in a much higher saturation stress (~270 MPa) than the 2 MeV Xe irradiation (~20 MPa) due to the smaller nuclear stopping. Using the stress map in Fig. 3 we can now predict the final saturation stress in SiO_2 for any irradiation condition (energy, ion) at 115 K up to several MeV. Since the temperature dependence of both the anisotropic strain generation rate A and the radiation-induced viscosity η_{rad} are known,[7] stress maps for SiO_2 at other temperatures can also be made. Finally, since η_{rad} and A have been determined for other materials as well,[10–12] stress maps for these materials may also be constructed.

In conclusion, we have calculated the depth-dependent mechanical stress induced by the interplay between densification by structural transformation, Newtonian viscous flow, and anisotropic strain generation in a constrained SiO_2 film, by taking into account the electronic and nuclear stopping dependence of these processes. Throughout the depth, the local stress shows variations as large as several hundred MPa, ranging between compressive and tensile. Finally, we have constructed a stress map that can predict the final saturation stress in SiO_2 at any depth in the film for any irradiation condition up to several MeV.

This work is part of the research program of FOM and was financially supported by NWO.

[1] A. Misra, S. Fayeulle, H. Kung, T. E. Mitchell, and M. Nastasi, Appl. Phys. Lett. **73**, 891 (1998).
[2] C. A. Volkert, J. Appl. Phys. **70**, 3521 (1991).
[3] E. Snoeks, T. Weber, A. Cacciato, and A. Polman, J. Appl. Phys. **78**, 4723 (1995).
[4] R. A. B. Devine, Nucl. Instrum. Methods Phys. Res. B **91**, 378 (1994).
[5] C. A. Volkert and A. Polman, Mater. Res. Soc. Symp. Proc. **235**, 3 (1992).
[6] H. Trinkaus and A. I. Ryazanov, Phys. Rev. Lett. **74**, 5072 (1995).
[7] M. L. Brongersma, E. Snoeks, T. van Dillen, and A. Polman, J. Appl. Phys. **88**, 59 (2000).
[8] A. Benyagoub, S. Löffler, M. Rammensee, S. Klaumünzer, and G. Saemann-Ischenko, Nucl. Instrum. Methods Phys. Res. B **65**, 228 (1992).
[9] D. L. Griscom, M. E. Gingerich, and E. J. Friebele, Phys. Rev. Lett. **71**, 1019 (1993).
[10] E. Snoeks, K. S. Boutros, and J. Barone, Appl. Phys. Lett. **71**, 267 (1997).
[11] S. Klaumünzer, Radiat. Eff. Defects Solids **110**, 79 (1989).
[12] M.-D. Hou, S. Klaumünzer, and G. Schumacher, Phys. Rev. B **41**, 1144 (1990).